sustainability

MDPI

Article

Voltage Zoning Regulation Method of Distribution Network with High Proportion of Photovoltaic Considering Energy Storage Configuration

Fangfang Zheng [1], Xiaofang Meng [1,*], Tiefeng Xu [1], Yongchang Sun [2] and Nannan Zhang [1]

[1] College of Information and Electric Engineering, Shenyang Agricultural University, Shenyang 110866, China; 15542178411@163.com (F.Z.); 15840578691@163.com (T.X.); zhangnannan@syau.edu.cn (N.Z.)

[2] Economic and Technological Development Zone Heating Limited Company, Dalian 116600, China; xielaoban1118@gmail.com

* Correspondence: xfmeng123@syau.edu.cn; Tel.: +86-158-0244-6563

Abstract: Photovoltaics have uncertain characteristics. If a high proportion of photovoltaics are connected to the distribution network, the voltage will exceed the limit. In order to solve this problem, a voltage regulation method of a distribution network considering energy storage partition configuration is proposed. Taking the minimum total voltage deviation, the minimum total cost, the minimum total power loss, and the minimum energy storage device installation ratio as the objective function, and considering various conditions, such as voltage deviation constraint and energy storage constraint, a mathematical model of voltage regulation is established. Firstly, a high proportion of photovoltaics are connected to the distribution network, and the voltage deviation curve is obtained. The optimal k value is determined by the elbow rule. The voltage deviation curve of each node is clustered by the k-means algorithm so as to determine the energy storage device partition. The energy storage device is connected to various clustering centers, and then the weighting factor of each objective function is determined by the fuzzy comprehensive evaluation method. For comparison and analysis, $(k + 1)$ schemes are determined through the partition configuration of $(k + 1)$ energy storage devices. Then, the model is solved by particle swarm optimization, and the unit output result and the minimum objective function value are obtained. Finally, an example of IEEE33 is used to verify the effectiveness of the proposed model.

Keywords: high proportion photovoltaic; voltage regulation; k-means clustering; energy storage partition; particle swarm optimization algorithm

check for updates

Citation: Zheng, F.; Meng, X.; Xu, T.; Sun, Y.; Zhang, N. Voltage Zoning Regulation Method of Distribution Network with High Proportion of Photovoltaic Considering Energy Storage Configuration. *Sustainability* **2023**, *15*, 10732. https://doi.org/10.3390/su151310732

Academic Editors: Xiang Li, Rohitha Weerasinghe and Raouf Mobasheri

Received: 5 June 2023
Revised: 6 July 2023
Accepted: 6 July 2023
Published: 7 July 2023

1. Introduction

Nowadays, the shortage of traditional energy is increasing, and the demand for energy is increasing. With this problem, the proportion of photovoltaic units (PV) connected to the grid is increasing [1–3], and the mismatch of source and load will also affect the voltage of the distribution network. For example, it is easy to have reverse power transmission during the peak period of PV output, which leads to the voltage exceeding the upper limit. The energy storing device (ESD) has the ability to suppress power fluctuation, which can effectively alleviate the mismatch between source and load [4]. Therefore, the voltage regulation technology of a distribution network compatible with PVs and ESDs came into being [5,6]. How to effectively plan a large number of PVs, other distributed power sources, and energy storage in the distribution network to reduce voltage deviation, cost, and power loss has become an urgent problem that needs a solution.

In recent years, many scholars and research institutions at home and abroad have studied the voltage regulation of distribution networks with PVs and have achieved results. Reference [7] analyzed the voltage and reactive power/active power regulation of photovoltaic access points and then put forward a reactive power/active power coordinated control method, which alleviated the voltage over-limit problem of a distribution network with distributed PVs; however, the economic cost was not considered in the model. Reference [8] put forward a double-layer optimization model in which the sensitivity analysis of dynamic comprehensive reactive power and voltage correction was considered. It was proved by examples that the model could reduce the peak–valley difference of load and improve the system voltage level. Reference [9] took the minimum voltage deviation and fluctuation as the objective function and combined traditional reactive power control equipment with PV multi-operation state regulation ability and put forward a voltage coordination control method. It was verified by a 21-node 10 kV actual system that this method could better improve the voltage regulation ability of a distribution network with PVs and improve the voltage safety level; however, energy storage and other distributed power sources were not considered in this paper. Reference [10] proposed a two-stage distributed robust opportunity using a constrained rolling time domain voltage control method, which was proved to be effective by an example of an unbalanced IEEE-123 system, but the energy storage device was also not considered in this paper. Reference [11] took the minimum investment cost as the objective function, established a distribution system voltage optimization model based on second-order cone programming, and used the MOSEK solver to solve the model. It was proved by the IEEE33 example that the model could effectively alleviate the voltage problem, but the change of branch network loss was not considered in the model. The voltage regulation of distribution network with a high proportion of PV still needs further study.

Aiming at the problem of distributed network voltage regulation (DNVR) in distribution networks with a high proportion of PVs, a DNVR model considering the ESD and high proportion of PVs is proposed, and nodes are clustered based on a k-means algorithm so that the ESD can be configured in different zones. Then, the particle swarm optimization (PSO) algorithm is used to solve the model. Finally, IEEE33 is used to illustrate the method proposed in this paper, which can improve voltage stability and operation economy on the basis of ensuring the safe operation of a distribution network. The main contributions of this work are summarized as follows:

(1) Based on the k-means clustering method, the voltage deviation curves of each node in a day are clustered and analyzed, and the nodes are divided into several categories to determine the distribution network partition. The ESDs are connected to the cluster centers of each district, thus realizing the voltage partition adjustment;
(2) The solution method based on PSO can effectively solve the proposed voltage regulation model;
(3) Based on the proposed voltage regulation method of a distribution network considering energy storage configuration, the IEEE33 example is analyzed, and the objective function values are effectively reduced, thus improving the stability and economy of the distribution network.

2. Partition Configuration of Energy Storage Based on K-Means Clustering

A high proportion of PVs connected to the grid leads to problems, such as voltage over the limit and power fluctuation. Therefore, the ESD is connected to the distribution network to realize voltage regulation. How to configure the ESD is the key. In this paper, the voltage deviation curve of each node is clustered by the k-means algorithm to realize the partition configuration of ESDs.

2.1. Definition of High Proportion

When a high proportion of PVs are connected to the distribution network, it will change the topology of the network and also have a certain impact on the power flow, thus changing the voltage distribution [12]. In this paper, the proportional definition of the PV grid connection is as follows:

$$\lambda = \frac{\sum P_{\mathrm{PV}}}{P_{L,\max}} \times 100\% \tag{1}$$

where P_{PV} is the total active power of PV connected to the system, kW; $P_{L,\max}$ is the peak load active power of the system, kW.

2.2. K-Means Clustering

In this paper, the k-means clustering algorithm is selected as the clustering method. It has the following advantages:

(1) Simple principle, easy realization and fast convergence;
(2) Good clustering effect;
(3) Strong interpretability and intuition;
(4) There is only one parameter, k.

The k-means clustering algorithm can divide the data of unknown tags into different groups according to their characteristics [13,14]; each group of data is also called a "cluster", and the center point of each cluster is called a "centroid". Its basic principal process is as follows:

(1) Randomly selecting k sample points as initial clustering centers;
(2) Calculating the distance between each cluster center and other sample points by using Euclidean distance and classifying each sample point into the nearest class;
(3) Finding a new cluster center of each class, and taking it as the center to calculate the average value of each class by Equation (2);

$$M_k = \frac{1}{N_k}\sum_{i=1}^{N_k} D_{ki} \tag{2}$$

where M_k is the center of class k; D_{ki} is the ith data in the kth class; N_k is the number of samples in each category.
(4) Repeating (2) and (3) until the clustering center does not change.

2.3. Elbow Rule to Determine the k Value

The selection of a k value is very important. This paper adopts the elbow rule to realize the selection of the k value. With the increase of cluster number k, the sum of squared errors (SSE) will also change, and the elbow rule is used to determine the optimal cluster number through the change trend of SSE [15]. SSE refers to the sum of squares of the distances from each data point to the center of its cluster, and its calculation formula is shown in Equation (3):

$$\mathrm{SSE} = \sum\nolimits_{i=1}^{k} \sum\nolimits_{p \in C_i} |p - m_i|^2 \tag{3}$$

where k indicates the number of clusters; C_i represents the ith cluster; p represents the sample point in C_i; m_i represents the average value of all data in the ith cluster.

When the cluster number k is small, SSE will gradually decrease; however, when the cluster number k continues to increase, the decline speed of SSE will gradually slow down until it finally becomes stable. At this time, the change trend of SSE presents a shape similar to an elbow, and the k value corresponding to the elbow is the best k value.

2.4. Partition Configuration of ESD

By calculating the power flow after a high proportion of PV nodes is connected to the grid, the voltage deviation results of each node are obtained. Then, the voltage deviation curve of each node's k-means clustering are obtained. The nodes can be divided into k categories so that the distribution system can be divided into k zones and the cluster center of each zone is selected to install the ESD so as to realize the ESD partition configuration.

3. Distribution Network Voltage Regulation Model with High Proportion of PV

In order to make the effect of DNVR better, we should consider not only the total voltage deviation of nodes but also the total power loss of branches, economic cost and

ESD installation ratio. Because there are a large number of PVs in the model, its output is uncertain, and the load output fluctuates [16,17]. It may change the power flow of the distribution network, and problems such as voltage exceeding limit and power fluctuation may occur, thus threatening the security of the power grid. Voltage regulation is an important link to effectively ensure the safe and stable operation of the power grid.

3.1. Objective Function

Micro turbines (MT) and a large number of PVs are connected to the DNVR model, and a distributed ESD is connected to stabilize the fluctuation [18]. In this paper, the regulation objective function is established from four aspects: reducing total voltage deviation, reducing total power loss, reducing economic cost and reducing the ESD installation ratio so as to realize DNVR with a high proportion of PVs, thus improving the economy and stability of the distribution network.

Objective function F_1: the total voltage deviation of nodes U_{dev_total} is the lowest [19,20]:

$$F_1 = \min \sum_{t=1}^{T} \sum_{i=1}^{N_{\text{node}}} \left| \frac{U_{i,t} - U_N}{U_N} \right| \tag{4}$$

where N_{node} is the number of independent nodes; T is the number of time periods; $U_{i,t}$ is the voltage amplitude of node i at time t, kV.

(1) Objective function F_2: the economic cost C_{E_total} is the lowest: C_{E_total} consists of ESD call cost C_{ESD}, power generation cost of PVs $C_{\text{PV},m}$, power generation cost of MTs $C_{\text{MT},ge}$, electricity purchase cost $C_{e,buy}$ [21] and environmental treatment cost C_{pt}, namely

$$C_{E\_total} = C_{\text{ESD}} + C_{\text{PV},ge} + C_{\text{MT},ge} + C_{e,buy} + C_{pt} + C_{nl} \tag{5}$$

① ESD call cost C_{ESD}

$$C_{\text{ESD}} = \mu_{\text{ESD}} P_{\text{ESD},c} + \mu_{\text{ESD}} P_{\text{ESD},dc} \tag{6}$$

where μ_{ESD} refers to the call cost of ESD unit power, yuan/kW.

② Power generation cost of PVs: PVs are clean energy, so there is no fuel cost, so $C_{\text{PV},ge}$ only consists of the operation and maintenance cost of PVs $C_{\text{PV},om}$.

$$C_{\text{PV},ge} = C_{\text{PV},om} = \sum_{t=1}^{T} c_{\text{PV},om} P_{\text{PV}}(t) \tag{7}$$

where $c_{\text{PV},om}$ is the unit operation and maintenance cost of PV, yuan/kW; $P_{\text{PV}}(t)$ is the PV output at time t, kW.

③ Power generation cost of MTs: $C_{\text{MT},ge}$ consists of fuel cost and operation and maintenance cost $C_{\text{MT},om}$ (see Equation (8)). Among them, $C_{\text{MT},fu}$ is related to factors such as natural gas price and power supply efficiency of the unit [22], and its calculation formula is shown in Equation (9). The calculation formula of $C_{\text{MT},om}$ is shown in Equation (10).

$$C_{\text{MT},ge} = C_{\text{MT},fu} + C_{\text{MT},om} \tag{8}$$

$$C_{\text{MT},fu} = \sum_{t=1}^{T} \frac{(3600/4.1868) \times c_{gas}}{Q_{gas}\eta} \cdot P_{\text{MT},i}(t) \tag{9}$$

$$C_{\text{MT},om} = \sum_{t=1}^{T} \sum_{i=1}^{N_{\text{MT}}} c_{\text{MT},om} P_{\text{MT},i}(t) \tag{10}$$

where c_{gas} is the price of natural gas, yuan/m^3; Q_{gas} is the power generation for natural gas, kcal/m^3; η is the power supply efficiency for the unit, %; $P_{\text{MT}}(t)$ is the

MT output at time t, kW; $c_{\mathrm{MT},om}$ is the unit operation and maintenance cost of MTs, yuan/kW.
④ Electricity purchase cost $C_{e,buy}$

$$C_{e,buy} = \sum_{t=1}^{T} \left(p_{ph}(t) \cdot P_{ee}(t) \right) \tag{11}$$

where $p_{ph}(t)$ is the electricity price purchased from the superior power grid at time t, yuan/kW; $P_{ee}(t)$ is the exchange power for the electric energy at time t, kW.
⑤ Environmental treatment cost C_{pt}: CO_2 and NO_x emissions come from MTs [23]. The calculation formula of C_{pt} is shown in Equation (12).

$$C_{pt} = \sum_{t=1}^{T} c_{po,k} \sigma_{po,k} P_{\mathrm{MT},i} \tag{12}$$

where $c_{po,k}$ are the emission cost coefficients of ith pollutants, respectively, yuan/kg; $\sigma_{po,k}$ is the discharge amount of ith pollutant, kg/kW.

(2) Objective function F_3: the total power loss of the branch ΔA_{nl_total} is the lowest.

$$F_3 = \min \sum_{t=1}^{T} \sum_{i=1}^{b} 10^{-3} \times \frac{\left(P_i^2(t) + Q_i^2(t)\right) R_i}{U_i^2(t)} \Delta t \tag{13}$$

where b is the number of branches; $P_i(t)$ and $Q_i(t)$ are, respectively, the active power (kW) and reactive power (kVar) flowing through branch i at time t; $U_i(t)$ is the terminal node voltage of branch i at time t, kV; R_i is the resistance value on branch i; Δt is the duration of each period, h.

(3) Objective function F_4: the installation ratio $\gamma_{\mathrm{ESD,rate}}$ of ESD is minimum.

$$F_4 = \min \frac{\sum_{i=1}^{N_{\mathrm{ESD}}} E_{\mathrm{ESD},i}}{\sum_{i=1}^{N_{\mathrm{PV}}} E_{\mathrm{PV},i}} \times 100\% \tag{14}$$

where N_{ESD} is the number of ESDs installed; N_{PV} is the number of installed PVs; $E_{\mathrm{ESD},i}$ is the capacity of the ith ESD, kW h; $E_{\mathrm{PV},i}$ is the capacity of the ith PV, kW h.

3.2. Constraints

The regulation model needs to meet equality conditions, such as power balance constraints and some inequality conditions, such as unit output constraints, voltage constraints, energy storage operation constraints and power purchase constraints.

3.2.1. Power Balance Constraints

The sum of the output of all units is equal to the sum of load power and power loss [24], namely:

$$\begin{cases} P_{\mathrm{g}}(t) + P_{\mathrm{PV}}(t) + P_{\mathrm{MT}}(t) + P_{\mathrm{ESD},dc}(t) - P_{\mathrm{ESD},c}(t) = P_{\mathrm{L}}(t) + P_{\mathrm{loss}}(t) \\ Q_{\mathrm{g}}(t) + Q_{\mathrm{MT}}(t) = Q_{\mathrm{L}}(t) + Q_{\mathrm{loss}}(t) \end{cases} \tag{15}$$

where $P_g(t)$ and $Q_g(t)$ are the active power (kW) and reactive power (kVar) of the power supply at time t, respectively; $P_{\mathrm{MT}}(t)$ and $Q_{\mathrm{MT}}(t)$ are, respectively, the active power (kW) and reactive power (kVar) emitted by the MTs at time t; $P_{\mathrm{ESD},dc}(t)$ and $P_{\mathrm{ESD},c,i}(t)$ are, respectively, the discharge and charging power of ESD at time t, kW; $P_L(t)$ and $Q_L(t)$ are, respectively, the active power (kW) and reactive power (kVar) of the load at time t;

$P_{\text{loss}}(t)$ and $Q_{\text{loss}}(t)$ are, respectively, the active power (kW) and reactive power (kW) of the network loss at time t.

3.2.2. Unit Output Constraints

The output of the unit meets the following constraints:

$$P_{i,\min} \le P_i(t) \le P_{i,\max} \tag{16}$$

where $P_{i,\max}$ and $P_{i,\min}$ are, respectively, the maximum and minimum value of active output of unit i, kW.

3.2.3. Voltage Constraints

The node voltage and voltage deviation satisfy the following constraints:

$$\begin{cases} U_i^{\min} \le U_i(t) \le U_i^{\max} \\ U_{dev}^{\min} U_N \le U_{dev}(t) \le U_{dev}^{\max} U_N \end{cases} \tag{17}$$

where $U_i^{\max}$ and $U_i^{\min}$ are, respectively, the maximum value and minimum value of the voltage amplitude of the ith node, kV; $U_{dev}^{\max}$ and $U_{dev}^{\min}$ are, respectively, the maximum value and minimum value of allowable voltage deviation of the ith node, %.

3.2.4. Energy Storage Operation Constraints

The ESD meets the following operational constraints during operation [25]:

$$\begin{cases} 0 \le P_{\text{ESD},c}(t) \le u_{\text{ESD},c}(t) P_{\text{ESD},c}^{\max} \\ 0 \le P_{\text{ESD},dc}(t) \le u_{\text{ESD},dc}(t) P_{\text{ESD},dc}^{\max} \\ u_{\text{ESD},c}(t) + u_{\text{ESD},dc}(t) \le 1 \\ \text{SOC}_{\min} \le \text{SOC}(t) \le \text{SOC}_{\max} \end{cases} \tag{18}$$

where $P_{\text{ESD},c}(t)$ and $P_{\text{ESD},c}^{\max}$ are, respectively, the charging power of ESD at time t and the maximum value of the charging power, kW; $P_{\text{ESD},dc}(t)$ and $P_{\text{ESD},dc}^{\max}$ are, respectively, the discharge power of ESD at time t and the maximum value of the discharge power, kW; $u_{\text{ESD},c}(t)$ and $u_{\text{ESD},dc}(t)$ are, respectively, the charging and discharging state of ESD at time t, which are variables of 0 to 1, $u_{\text{ESD},c}(t) = 1$ indicating that ESD is in a charging state and $u_{\text{ESD},dc}(t) = 1$ indicating that ESD is in a discharging state; $\text{SOC}(t)$ is the state of charge of ESD at time t, kVA; $\text{SOC}_{\max}$ and $\text{SOC}_{\min}$ are, respectively, the maximum and minimum values of ESD state of charge, kVA.

3.2.5. Power Purchase Constraints

The power purchased meets the following constraints:

$$0 \le P_{ee}(t) \le P_{ee,\max} \tag{19}$$

where $P_{ee,\max}$ is the maximum value of electric energy exchange power, kW.

3.3. Mathematical Model of Voltage Regulation

The magnitude difference between objective functions is very large, and the dimensions are inconsistent, which will affect the results of DNVR if it is not processed. In order to eliminate this influence, it is necessary to standardize all indicators, among which the most typical one is normalization [26]. In this paper, the maximum–minimum normalization method is used to map the data values of each index to [0, 1]. Set F_n' as the objective function after normalization, and the calculation formula is as follows:

$$F_n' = \frac{F_n - F_{n,\min}}{F_{n,\max} - F_{n,\min}} \tag{20}$$

where F_n is the ith objective function, $n = 1,2,3,4$; $F_{n,\max}$ and $F_{n,\min}$ are, respectively, the maximum and minimum values of F_n.

Then, the mathematical model of DNVR with a high proportion of PVs is:

$$\min F = m_1 F_1' + m_2 F_2' + m_3 F_3' + m_4 F_4' \tag{21}$$

where m_1, m_2, m_3 and m_4 are, respectively, the weighting factor of F_1', F_2', F_3' and F_4', and they satisfy $m_1 + m_2 + m_3 + m_4 = 1$.

3.4. Determination of the Weighting Factor of the Objective Function

In this paper, the fuzzy comprehensive evaluation method (FCE) is used to determine the weighting factor of each objective factor in Section 3.3 [27], and its calculation steps are as follows:

Step (1): Calculate the overweight weighted value m_n' of each factor, and the calculation formula is as follows:

$$m_n' = \frac{d_{ac,n}}{d_{ma,n}} \tag{22}$$

where $d_{ac,n}$ is the actual value of the nth factor (usually taking the averaged value), $n = 1,2,3,4$; $d_{ma,n}$ is the maximum allowable value of the nth factor (usually taking the maximum value).

Step (2): Calculate the weighting factor of each factor as follows:

$$m_n = \frac{m_n'}{\sum\limits_{n=1}^{N_F} m_n'} \tag{23}$$

where N_F is the number of objective functions.

4. Mathematical Model Solving Method

In this paper, PSO is used to solve the DNVR model [28]. PSO is a kind of collective intelligence algorithm designed by imitating the predatory behavior of birds. Assuming that there is only one piece of food in the area (usually the best solution to the optimization problem), the task of birds is to find this source. In the whole research process, by transmitting their own information to each other, other birds can know their position through this cooperation to determine whether they have found the best solution. Finally, by transmitting the best information to the whole bird, the whole bird can gather around the food source, which is the best solution, that is, the optimal solution of the problem. The foraging behavior of birds corresponds to the algorithm principle, as shown in Table 1. The optimal output of each unit and the optimal value of each objective function can be obtained through PSO.

Table 1. Correspondence between foraging behavior of birds and algorithm principle.

Behavior	PSO
Bird	Particle
Forest	Solution space
The amount of food	Objective function value
The position of each bird	A solution in space (Particle position)
The postion with the most food	Global optimal solution

PSO is initialized as a group of random particles, and the optimal solution is found through iteration. In each iteration, the particle updates its position and velocity by tracking two extreme values: one is the optimal solution found by the particle itself, which is called individual extreme value; the other is the optimal solution found by the whole population at present, which is called the global extreme value. Among them, the formula for updating position and speed is as follows [29]:

$$V_i^{t+1} = \omega V_i^t + r_1 p(P_i^t - x_i^t) + r_2 p(G_i^t - x_i^t) \tag{24}$$

$$X_i^{t+1} = X_i^t + V_i^{t+1} \tag{25}$$

where V_i^t is the velocity of the ith particle in the tth iteration; p is a random number between 0 and 1; r_1 is a self-learning factor; r_2 is a global learning factor; ω is the inertia weight; X_i^t is the position of the ith particle in the tth iteration.

The traditional particle swarm optimization algorithm uses a fixed ω, which affects the global search and convergence speed [30]. Using variable ω can improve the global and local optimization performance of the algorithm, and its calculation formula is as follows:

$$\omega = \frac{\omega_{\max} d_{\max}^2 - (\omega_{\max} - \omega_{\min}) d^2}{d_{\max}^2} \tag{26}$$

where $\omega_{\max}$ and $\omega_{\min}$ are, respectively, the maximum and minimum value of inertia weight; d is the current iteration number; $d_{\max}$ is the maximum number of iterations.

5. Example Analysis

5.1. Basic Data

In this paper, the programming is based on MATLAB (version is R2016a), and the IEEE33-node system is taken as an example. This system is a classic distribution network model abstractly equivalent from the actual system, and it is a typical radiation network model. The system diagram is shown in Figure 1 (numbers in Figure 1, such as 1, 2, 3, etc., are node serial numbers.); the voltage reference value U_B is 12.66 kV; the power reference value S_B is 100 MVA, and the network parameters are shown in Reference [12]. Select the PV and load data of the maximum load day in a certain area in summer for analysis (see Figure 2). A high proportion of PVs are connected at nodes 10, 11 and 12 (the proportion of PV connection is 72.4% in this calculation example), and the MT is connected at nodes 3 and 24, respectively. See Table 2 for the parameters of output power and voltage limit. The parameters involved in the cost function are shown in Tables 3 and 4. The electricity price curve is shown in Figure 3.

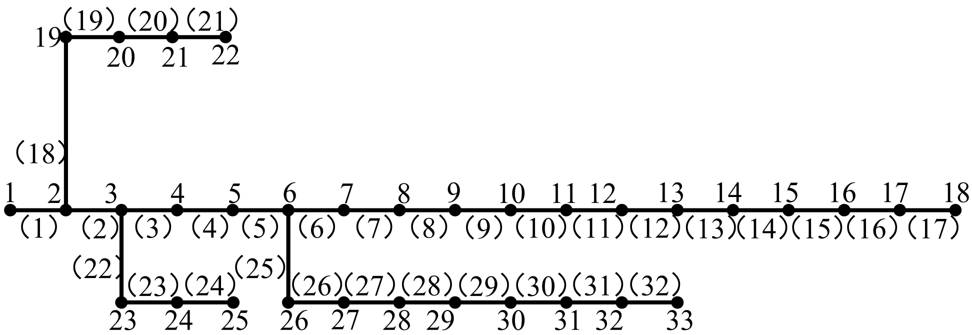

Figure 1. IEEE33 system diagram.

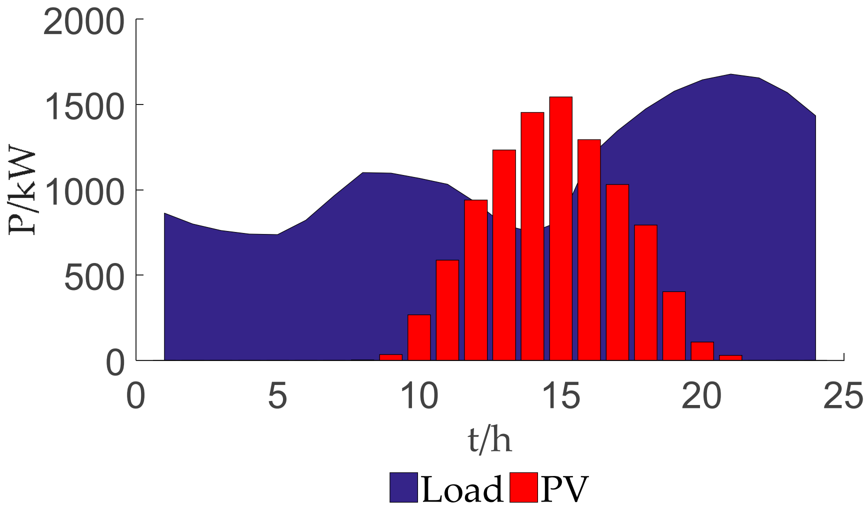

Figure 2. PV and load output.

Table 2. Constrains parameter setting.

Parameter	Value
$P_{i,\max}$	200
$P_{i,\min}$	100
$U_i^{\max}$	13.293
$U_i^{\min}$	11.394
$U_{dev}^{\max}$	0.633
$U_{dev}^{\min}$	−0.633
$P_{\mathrm{ESD},c}^{\max}$	−250
$P_{\mathrm{ESD},dc}^{\max}$	250
$P_{ee,\max}$	5000
$\mathrm{SOC}_{\max}$	1000
$\mathrm{SOC}_{\min}$	100

Table 3. Cost parameter setting.

Parameter	Value
μ_{ESD}	0.045
$c_{\mathrm{PV},om}$	0.0096
c_{gas}	2.20
Q_{gas}	8500
η	32
$c_{\mathrm{MT},om}$	0.082

Table 4. Environmental treatment cost parameter setting.

Pollutant Type	$c_{po,k}$	$\sigma_{po,k}$
CO_2	724	0.994
NO	0.0036	0.00653
NO_2	0.2	0.00312

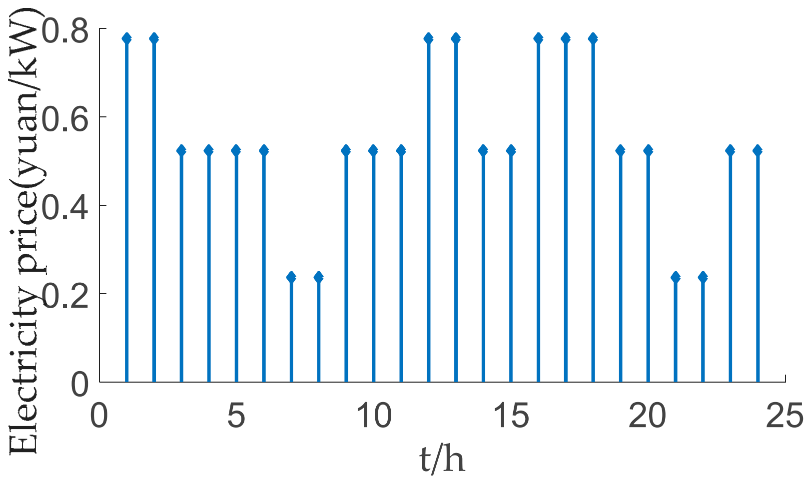

Figure 3. Time-sharing electricity price curve.

In order to verify the method proposed in this paper, firstly, the nodes are grouped into $(k - i)$ categories ($0 < i < k$, and i is an integer), and $(k - i)$ ESD with the same total capacity are, respectively, connected to various cluster centers, and $(k - 1)$ schemes are obtained. Then, according to the method proposed above, the nodes are grouped into k classes, and a scheme is determined. Then, the nodes are grouped into $(k + 1)$ categories to determine the last scheme. Connect ESD to each cluster center, respectively, and calculate DNVR results. To sum up, determine $(k + 1)$ scheme.

In PSO, the maximum number of iterations is 150, the dimension of search space is 144, the number of particles is 50, the maximum and minimum values of inertia weight are 0.9 and 0.4, respectively, and the learning factors c_1 and c_2 are both 2. The DNVR strategy based on the PSO algorithm proposed in this paper is used to adjust the voltage of this example to verify the effectiveness of the proposed model.

See Tables 5 and 6 for the parameter settings involved in the FCE method.

Table 5. Actual value data.

Actual Value	Value
$d_{ac,1}$/kV	2.0639
$d_{ac,2}$/yuan	3017.94
$d_{ac,3}$/kW	0.3368
$d_{ac,4}$/%	0.1056

Table 6. Maximum allowable value data.

Maximum Allowable Value	Value
$d_{ma,1}$/kV	2.5400
$d_{ma,2}$/yuan	3796.01
$d_{ma,3}$/kW	0.5549
$d_{ma,4}$/%	0.1234

5.2. Determine the Scheme

The weighting factor of each objective function can be calculated from Equation (22) and Equation (23), and the results are shown in Table 7.

Table 7. Weighting factor results of each objective function.

Weighing Factor	Value
m_1	0.2646
m_2	0.2590
m_3	0.1977
m_4	0.2787

In this paper, the Newton–Raphson method is used to calculate the power flow, and the power flow results before and after the high-proportion PV grid connection can be obtained, among which the voltage results are shown in Figure 4.

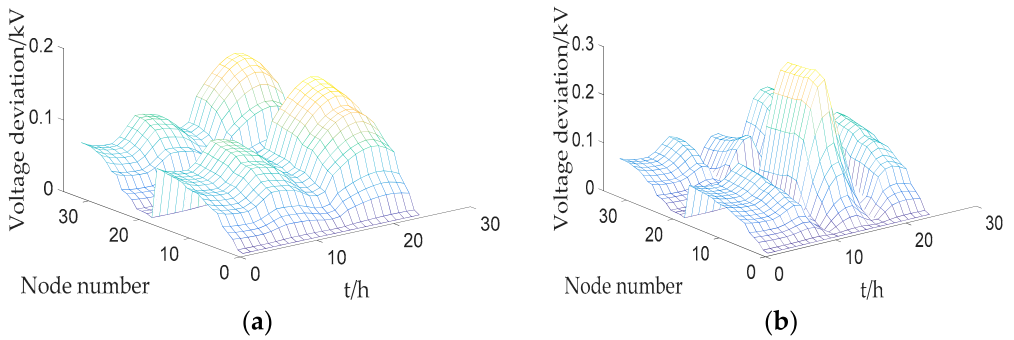

Figure 4. Voltage deviation curves: (**a**) before high proportion PV grid connection; and (**b**) after high proportion PV grid connection.

It can be found that after a high proportion of PV nodes are connected to the grid, the voltage of each node rises, and the voltage near the access point (such as nodes 10, 11 and 12) rises most obviously at noon and afternoon (that is, the peak period of PV output), and even the voltage exceeds the limit. k-means clustering is performed on the voltage deviation curve of each node, and the best k value is determined by the elbow rule. See Figure 5 for SSE curve.

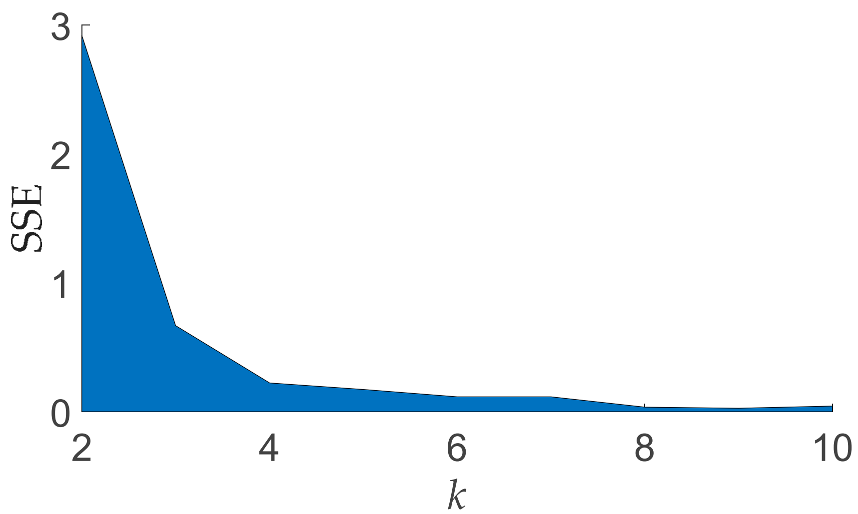

Figure 5. SSE curve.

Observing Figure 5, it can be seen that after k = 4, the SSE value basically does not change, and the SSE curve forms an "elbow" shape at k = 4, so 4 is selected as the best k value. Thus, 33 nodes are grouped into 4 categories, and the results are shown in Table 8.

Table 8. Node clustering results.

Cluster Sequence Number	Node Division	Cluster Center (Node Configured with ESD)
1	1, 2, 19~22	19
2	6~9, 26~33	8
3	10~18	13
4	3~5, 23~25	24

The system partition is shown in Figure 6.

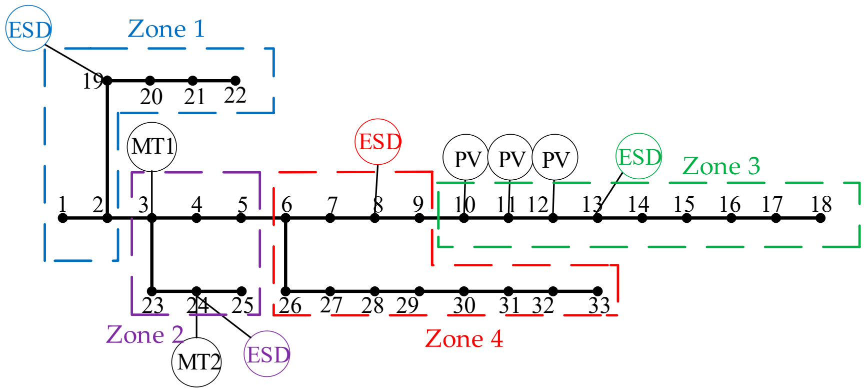

Figure 6. ESD four-zone configuration system diagram.

For comparative analysis, the nodes are grouped into 1, 2, 3 and 5 categories by using the k-means algorithm to determine 1, 2, 3 and 5 zones, respectively, and the ESD is also connected to the cluster center, respectively. See Figures 7–10 for the system diagram.

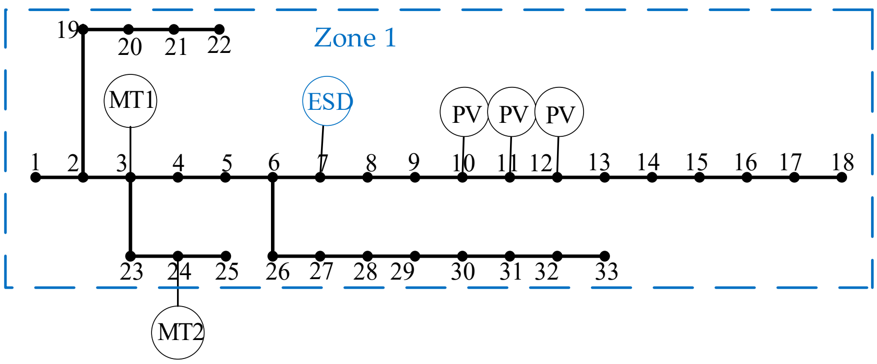

Figure 7. ESD one-zone configuration system diagram.

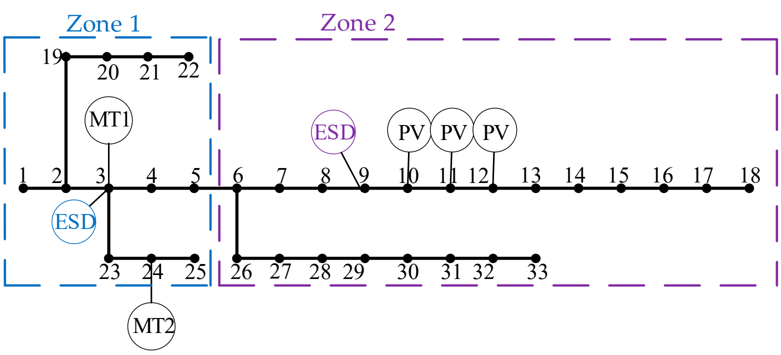

Figure 8. ESD two-zone configuration system diagram.

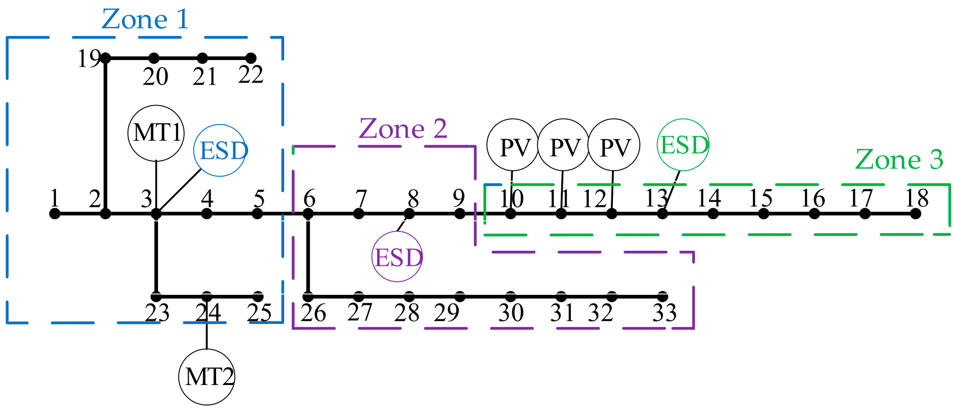

Figure 9. ESD three-zone configuration system diagram.

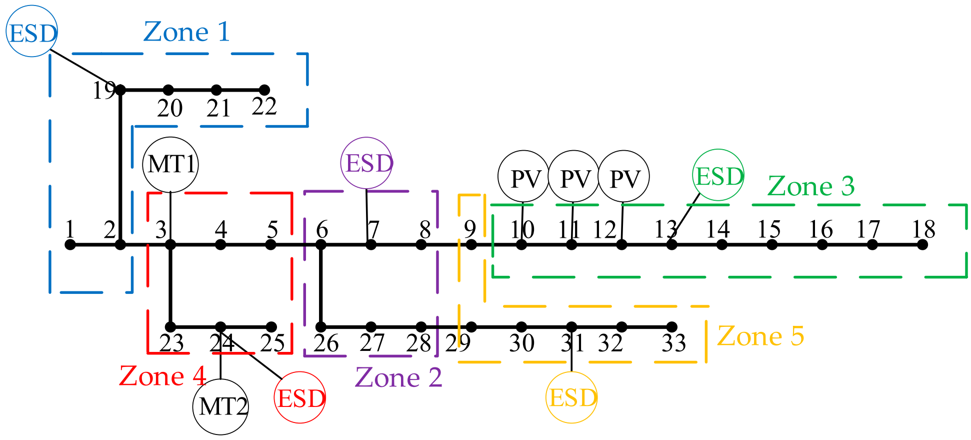

Figure 10. ESD five-zone configuration system diagram.

So as to determine the following five schemes:

Scheme 1: According to Figure 1, one ESD; with a capacity of 3.6 MWh are configured at nodes 7;

Scheme 2: According to Figure 8, two ESDs; each with a capacity of 1.6 MWh are configured at nodes 3 and 9;

Scheme 3: According to Figure 9, three ESDs; each with a capacity of 1 MWh are configured at nodes 3, 8 and 13;

Scheme 4: According to Figure 6, four ESDs; each with a capacity of 0.7 MWh are configured at nodes 19, 8, 13 and 24;

Scheme 5: According to Figure 10, five ESDs, each with a capacity of 0.56 MWh are arranged at nodes 19, 7, 13, 24 and 31.

5.3. DNVR Result Analysis Based on PSO

Using the PSO algorithm to solve the model, the output results of each unit and the results of each objective function at each time are obtained. Among them, the results of the MT output, ESD output and voltage deviation are shown in Figures 11–13, respectively.

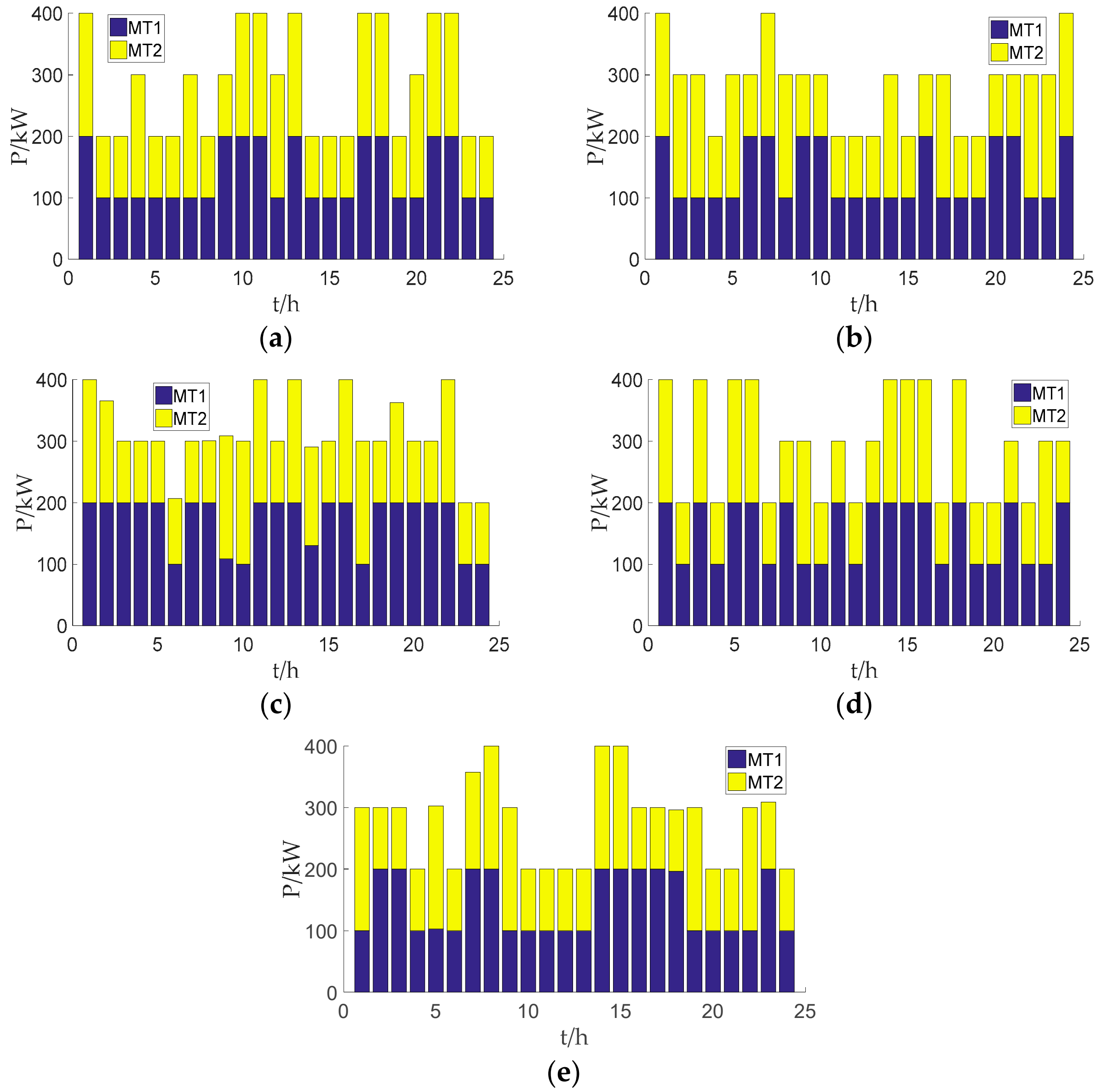

Figure 11. MT output results under various schemes (**a**) scheme 1; (**b**) scheme 2; (**c**) scheme 3; (**d**) scheme 4; (**e**) scheme 5.

See Table 9 for the specific cost results of each scheme after DNVR.

Table 9. Specific Results of Total Cost.

Subitem	C_{ESD}/Yuan	$C_{PV,ge}$/Yuan	$C_{MT,ge}$/Yuan	$C_{e,buy}$/Yuan	C_{pt}/Yuan
Before DNVR	0	280.0	0	40,315.1	0
scheme 1	270.0	280.0	6085.8	31,144.2	1311.1
scheme 2	540.0	280.0	5997.6	30,259.0	1292.0
scheme 3	769.7	280.0	6645.7	28,384.1	1431.6
scheme 4	1080.0	280.0	6262.2	25,538.2	1349.0
scheme 5	1280.8	280.0	5897.2	27,352.3	1266.5

The numerical comparison results of each objective function under each scheme are shown in Table 10.

Table 10. Total comparison results of each objective function.

Subitem	U_{dev_total}/kV	C_{E_total}/Yuan	A_{nl_total}/kWh	$\gamma_{ESD,rate}$/%
Before DNVR	48.1080	40,595	6.5324	0
scheme 1	35.6493	39,091	5.8300	12.34
scheme 2	35.1966	38,369	5.6184	10.97
scheme 3	34.0495	37,511	5.5829	10.29
scheme 4	32.3250	34,509	5.2677	9.60
scheme 5	33.8130	36,059	5.5074	9.60

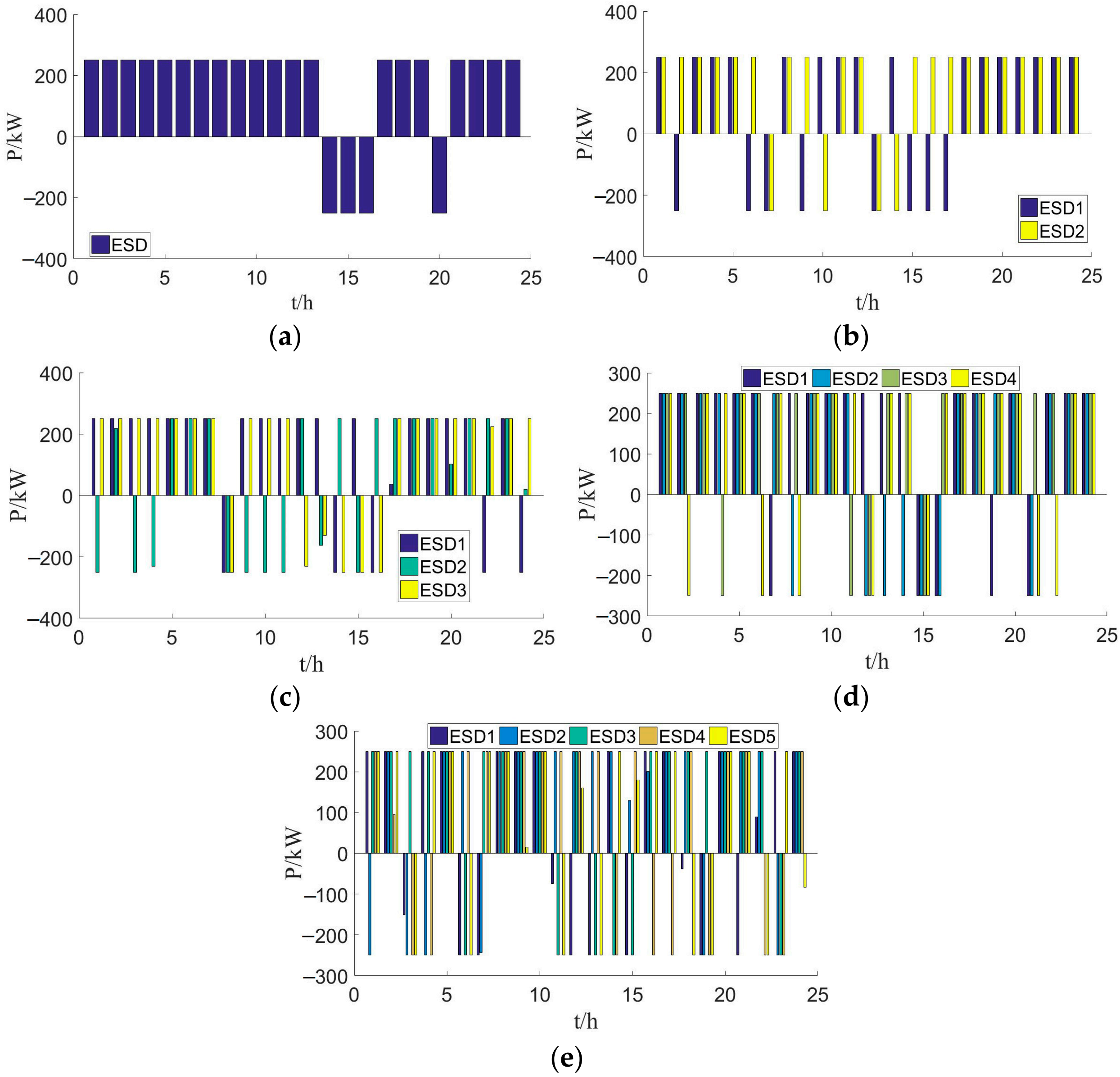

Figure 12. ESD output results under various schemes (**a**) scheme 1; (**b**) scheme 2; (**c**) scheme 3; (**d**) scheme 4; (**e**) scheme 5.

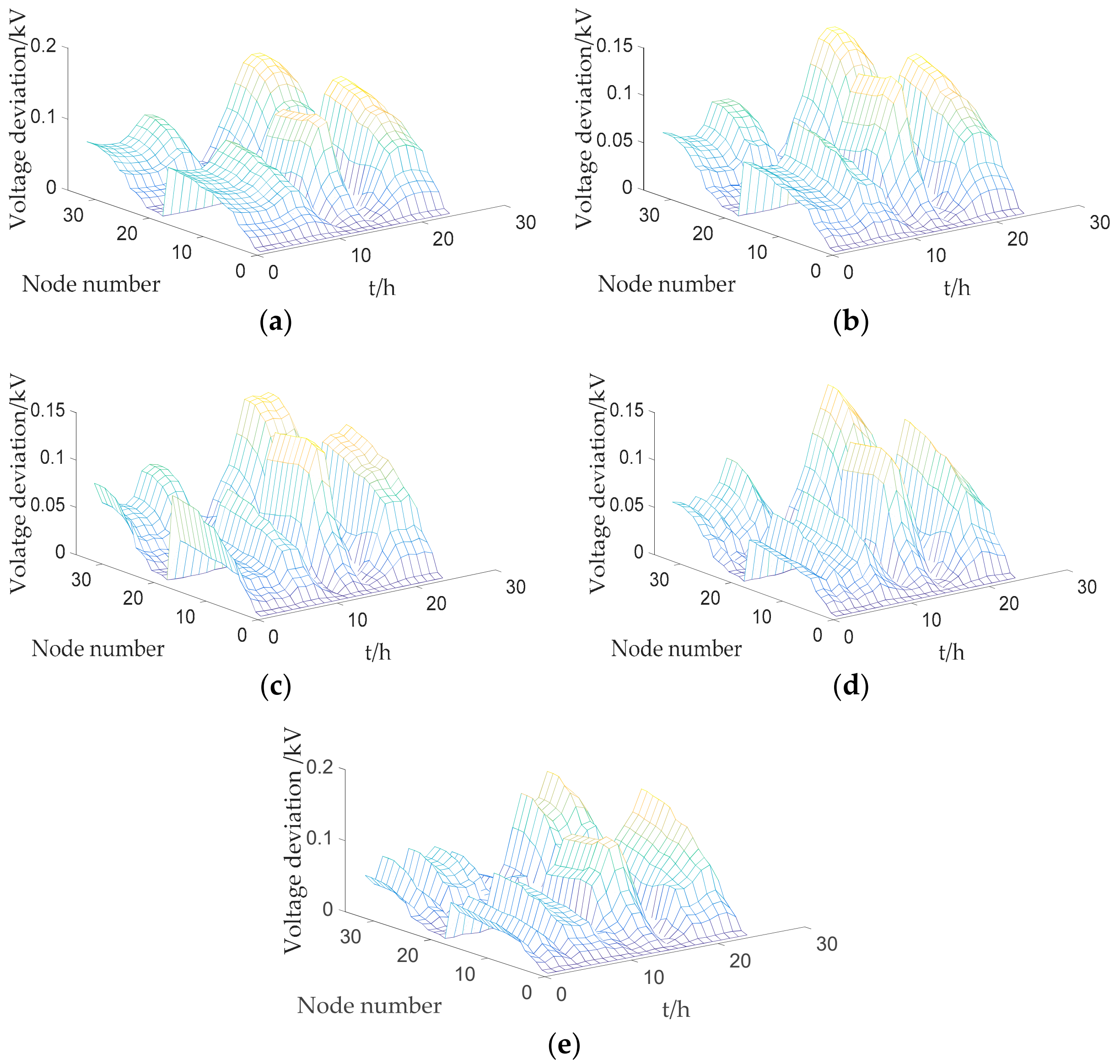

Figure 13. Voltage deviation results under various schemes (**a**) scheme 1; (**b**) scheme 2; (**c**) scheme 3; (**d**) scheme 4; (**e**) scheme 5.

Analyze with reference to Figures 11–13 and Tables 9 and 10:

Before DNVR: there is only PV in the system, and the ESD and MT are not connected at this time, so the call cost of the ESD, power generation cost of the MT, and environmental treatment cost are all zero; $C_{e,buy}$ is the highest, and C_{E_total} is also the highest compared with other schemes.

Scheme 1: The total output of the MT reaches the upper limit at 1:00, 10:00~11:00, 13:00, 17:00~18:00 and 21:00~22:00, and the output of the ESD always reaches the limit, and most are in the discharge state. Since the output of PV is fixed, $C_{\mathrm{PV},ge}$ is also fixed. After DNVR under scheme 1, C_{ESD} is the lowest, U_{dev_total} is reduced by 25.90%, C_{E_total} is reduced by 3.70%, and P_{nl_total} is reduced by 10.75%.

Scheme 2: The total output of the MT reaches the upper limit at 1:00, 7:00, 24:00, and both ESD outputs reach the limit at each time. After DNVR under scheme 2, U_{dev_total} is reduced by 26.84%, C_{E_total} is reduced by 5.48%, and P_{nl_total} is reduced by 13.99%.

Scheme 3: The total output of the MT is the most, so $C_{\mathrm{MT},ge}$ is the highest, and ESD is discharged most of the time. After DNVR under scheme 3, U_{dev_total} is reduced by 29.22%, C_{E_total} is reduced by 7.60%, and P_{nl_total} is reduced by 14.54%.

Scheme 4: The total output of the MT is relatively large, and most of the ESD is in a discharge state. After DNVR under scheme 4, U_{dev_total} is reduced by 32.81%, C_{E_total} is reduced by 14.99%, and P_{nl_total} is reduced by 19.36%.

Scheme 5: The total output of the MT is relatively minimum, and each ESD reaches the limit at all times. After DNVR under scheme 5, U_{dev_total} is reduced by 29.71%, C_{E_total} is reduced by 11.71%, and P_{nl_total} is reduced by 15.69%.

It can be found that the objective function values of these five schemes are effectively reduced compared with those before DNVR, which verifies the effectiveness of the mathematical model established in this paper. Among the five schemes, the closer the system partition is to the four zones, the better the effect of DNVR. Among them, the installation ratio of ESD $\gamma_{\mathrm{ESD,rate}}$ in scheme 1 is the largest, but the adjustment effect is still the worst, which shows that the effect of centralized access to the ESD is not as good as that of decentralized access to the ESD. The $\gamma_{\mathrm{ESD,rate}}$ in scheme 4 is equal to scheme 5 in ESD, and the lowest among several schemes, but the regulation effect of scheme 4 is still better than any other scheme, which verifies the effectiveness of the ESD partition configuration method based on node k-means clustering proposed in this paper.

6. Conclusions

In this paper, a DNVR model with a high proportion of PVs is established, and the model is solved by the PSO algorithm. The effectiveness of this method is verified based on the IEEE33-bus system. The conclusions are as follows:

(1) When establishing a DNVR model with the lowest total voltage deviation, the lowest total cost, including fuel cost, operation and maintenance cost, electricity purchase cost, and environmental treatment cost, the lowest total power loss, and the lowest installation ratio of the ESD as the goal, the model is relatively perfect. It can be more in line with the actual operation of a distribution network and has a good adjustment effect by comprehensively considering many constraints such as power flow constraints, voltage deviation constraints and energy storage constraints;

(2) After high-proportion PV access, node k-means clustering is performed on the voltage deviation curve of each node. The system is divided into different areas, and then FCE is used to determine the weighting factor of each objective function, thus making the determination of energy storage access location more reasonable and the subsequent adjustment effect better;

(3) The results of the PSO algorithm show that the calculation results of the proposed method can effectively adjust the voltage, reduce the cost, reduce the power loss and reduce the installation ratio of ESD, thus improving the economy and security of power grid operation.

The method proposed in this paper is suitable for distribution networks with energy storage devices, especially with a high proportion of photovoltaic units. Because the connection of wind turbines has not been considered in the mathematical model proposed in this paper, it needs to be further explored in future research to put forward a more effective voltage regulation scheme.

Author Contributions: Conceptualization, F.Z. and X.M.; methodology, X.M.; software, F.Z.; validation, F.Z., X.M. and T.X.; formal analysis, X.M.; investigation, T.X. and Y.S.; resources, T.X. and Y.S.; data curation, Y.S.; writing—original draft preparation, F.Z.; writing—review and editing, X.M.; visualization, N.Z.; supervision, X.M.; project administration, N.Z.; funding acquisition, N.Z. All authors have read and agreed to the published version of the manuscript.

Funding: This research was funded by Youth Program of National Natural Science Foundation of China (Grant number 61903264).

Institutional Review Board Statement: Not applicable.

Informed Consent Statement: Informed consent was obtained from all subjects involved in the study.

Data Availability Statement: Not applicable.

Conflicts of Interest: The authors declare no conflict of interest.

References

1. Li, B.; Chen, M.; Zhong, H.; Ma, Z.; Liu, D.; He, G. Review of Long-term Planning of New Power Systems with Large Share of Renewable Energy. *Proc. CSEE* **2023**, *43*, 555–581.
2. Wang, P.; Wu, Q.; Huang, S.; Zhou, B.; Li, C. Distributed optimal voltage control strategy for AC grid with DC connection and offshore wind farms based on ADMM. *Int. J. Electr. Power Energy Syst.* **2022**, *137*, 107802. [CrossRef]
3. Liu, J.; Hu, H.; Yu, S.S.; Trinh, H. Distributed Optimization Control Method of Virtual Energy Storage Plants for Power Grid Ancillary Services. *Autom. Electr. Power Syst.* **2022**, *46*, 181–188.
4. Liu, Z.; Liu, B.; Ding, X.; Wang, F. Research on optimization of energy storage regulation model considering wind–solar and multi-energy complementary intermittent energy interconnection. *Energy Rep.* **2022**, *8*, 490–501. [CrossRef]
5. Wang, J.; Wang, W.; Wang, H.; Wang, S.; Du, J. Two-stage coordinated planning of DG, SOP and ESS in an active distribution network considering violation risk. *Power Syst. Prot. Control* **2022**, *50*, 71–82.
6. Guo, C.X.; Liu, Z.P.; Feng, B.; Jiang, B.; Guo, J.; Liu, F. Research Status and Prospect of New-type Power System Risk Assessment. *High Volt. Eng.* **2022**, *48*, 3394–3404.
7. He, X.; Chen, Z.; Liu, X.; Zhang, T.; Chen, L. Voltage control strategy for medium voltage distribution network with distributed photovoltaic generators. *Electr. Meas. Instrum.* **2022**, *59*, 142–148.
8. Wang, Y.; Chen, Q.; Zheng, Y.; Xue, H.; Li, M.; Mi, Y. Optimal scheduling of mobile energy storage in active distribution network based on dynamic reactive power and voltage sensitivity. *Electr. Power Autom. Equip.* **2023**, *43*, 59.
9. Yang, G.; Sun, R.; Ding, R.; Xu, H.; Chen, C.; Wu, L.; Chen, Q.; Xia, M. Multi Time Scale Reactive Power and Voltage Optimization of Distribution Network Considering Photovoltaic Multi State Regulation Capability. *Electr. Power* **2022**, *55*, 105–114.
10. Zhang, Z.; da Silva, F.F.; Guo, Y.; Bak, C.L.; Chen, Z. Coordinated voltage control in unbalanced distribution networks with two-stage distributionally robust chance-constrained receding horizon control. *Renew. Energy* **2022**, *198*, 907–915. [CrossRef]
11. Pan, W.; Mao, M.; Zhou, Y.; Quan, X.; Li, Y. The impact of extreme weather condition on the voltage regulation in distribution systems with high penetration of roof-top photovoltaic. *Energy Rep.* **2021**, *7*, 320–331. [CrossRef]
12. Yang, S.; Li, Q.; Ming, Z.; Ma, Q.; Luo, Q. Multi-Objective Probabilistic Reactive Power Optimization of Distribution Network Considering the Randomness of Source and Load. *Southern Power Syst. Technol.* **2023**, *17*, 125–135.
13. Zheng, F.; Meng, X.; Wang, L.; Zhang, N. Operation Optimization Method of Distribution Network with Wind Turbine and Photovoltaic Considering Clustering and Energy Storage. *Sustainability* **2023**, *15*, 2184. [CrossRef]
14. Wu, Y.; Yao, L.; Liao, S.; Liu, Y.; Li, J.; Wang, X. A Peak Shaving Method of Aggregating the Distributed Photovoltaics and Energy Storages Based on the Improved K-means++Algorithm. *Power Syst. Technol.* **2022**, *46*, 3923–3931.
15. Zheng, F.; Meng, X.; Wang, L.; Zhang, N. Power Flow Optimization Strategy of Distribution Network with Source and Load Storage Considering Period Clustering. *Sustainability* **2023**, *15*, 4515. [CrossRef]
16. Wang, Z.; Ma, S.; Li, G.; Bian, J. Day-Ahead and Intra-Day Two-Stage Rolling Optimal Dispatch of Power Grid Considering Access of Composite Energy Storage Power Stations. *Acta Energiae Solaris Sin.* **2022**, *43*, 400–408.
17. Shen, J.; Wang, Y.; Cheng, C.; Li, X.; Miao, S.; Zhang, Y.; Zhang, J. Research Status and Prospect of Generation Scheduling for Hydropower-wind-solar Energy Complementary System. *Proc. CSEE* **2022**, *42*, 3871–3885.
18. Li, C.; Dong, Z.; Li, J.; Zhang, H.; Jing, Q.; Qian, K. Control Strategy of Voltage Regulation for Distributed Energy Storage Cluster in Distribution Network. *Autom. Electr. Power Syst.* **2021**, *45*, 133–141.
19. Wu, Y.; Cheng, X.; Liu, J. Distribution Network Reconfiguration Based on Hybrid Simulated Annealing Cuckoo Algorithm. *Sci. Technol. Eng.* **2023**, *23*, 626–632.
20. Huang, Z.; Chen, Y.; Mao, Z.; Sun, J.; Zha, X. Joint Access Planning of Soft Open Point and Distributed Energy Storage System. *Autom. Electr. Power Syst.* **2022**, *46*, 29–37.
21. Zhao, P.; Wu, J.; Zhang, W.; He, S.; Zhang, H. Cooperative Peer to Peer Scheduling of Multi-microgrids Considering Distribution Network Power Flow and Source-load Uncertainty. *Power Syst. Technol.* **2022**, *46*, 4885–4896. [CrossRef]
22. Tian, F.; Jia, Y.; Ren, H.; Bai, Y.; Huang, T. "Source-load" Low-carbon Economic Dispatch of Integrated Energy System Considering Carbon Capture System. *Power Syst. Technol.* **2020**, *44*, 3346–3355.
23. Huang, H.; Liang, R.; Zhang, X.; Lu, M.; Wang, C.; Zhang, G. Two-stage Multi-objective Deployment Optimization of Coal Mine Integrated Energy System Considering Carbon Emission Constraints. *Power Syst. Technol.* **2022**, *46*, 1731–1742.
24. Zhao, S.; Han, L.; Li, Z.; Yang, Y.; Ma, S. Day-ahead Optimal Scheduling of Active Distribution Network by Related Opportunity Goal Planning. *J. North China Electr. Power Univ.* **2021**, *48*, 1–10.
25. Cheng, Y.; Chen, X. Analysis on Influence of Energy Storage on Accommodation Capability of Wind Power Based on Source-Load-Storage Interaction. *Autom. Electr. Power Syst.* **2022**, *46*, 84–93.
26. Cheng, M.; Zhang, X.; Xu, M.; Xue, Y.; Wu, W.; He, Y. Loeation method of an active distribution network fault section based on multi-target weighted grey target decision. *Power Syst. Prot. Control* **2021**, *49*, 124–132.
27. Meng, X.; Wang, L.; Wang, X.; Wang, Y.; Liu, R.; Wang, H. Improve operation characteristics in three-phase four-wire low-voltage distribution network using distributed generation. *Power Syst. Technol.* **2018**, *2018*, 4091–4100.
28. Ma, Y.; Xie, J.; Zhao, S.; Wang, Z.; Luo, Z. Multi-objective Optimal Dispatching for Active Distribution Network Considering Park-level Integrated Energy System. *Autom. Electr. Power Syst.* **2022**, *46*, 53–61.

29. Yan, Q.; Dong, X.; Mu, J.; Ma, Y. Optimal configuration of energy storage in an active distribution network based on improved multi-objective particle swarm optimization. *Power Syst. Prot. Control* **2022**, *50*, 11–19.
30. Meng, R.; Zhao, J.; Zhou, T. Rapid Deployment Strategy of Emergency Repair Team Based on Improved Inertial Weighted PSO. *Power Syst. Clean Energy* **2021**, *37*, 17–24.